

# Numerical study of quantum Hall effect in two-dimensional multi-band system: single- and multi-layer graphene

Masao Arai<sup>a</sup>, Yasuhiro Hatsugai<sup>b</sup>

<sup>a</sup> Computational Materials Science Center, National Institute for Materials Science, Tsukuba, Ibaraki 305-0044, Japan

<sup>b</sup> Department of Physics, University of Tsukuba, Tsukuba, Ibaraki, 305-8571, Japan

## Abstract

The Chern numbers which correspond to quantized Hall conductance  $\sigma_{xy}$  were calculated for single- and bi-layer honeycomb lattices. The quantization of  $\sigma_{xy}$  occurs in entire energy range. Several large jumps of Chern numbers appear at van-Hove singularities of energy bands without magnetic fields. The plateaux of  $\sigma_{xy}$  are discussed from semi-classical quantization.

**Key words:** graphene, quantum Hall effect

**PACS:** 73.43.-f, 73.21.-b, 03.65.Sq

## 1. Introduction

The quantum Hall effect (QHE) is one of the most peculiar phenomena in two-dimensional electron system. The quantized Hall conductance  $\sigma_{xy}$  has been widely accepted as a topological quantity [1, 2, 3, 4, 5, 6, 7, 8]. When the chemical potential is located within an energy gap, the  $\sigma_{xy}$  is given as

$$\sigma_{xy} = -\frac{e^2}{h}c_F, \quad (1)$$

where  $c_F$  is a Chern number, which is an topological integer defined for occupied states. The  $c_F$  has been computed for simple tight-binding models and exotic nature of electron states under uniform magnetic field has been revealed.

Recently, the discovery of anomalous QHE in graphene [9, 10] shed a new light to the quantization of Hall conductance. The  $\sigma_{xy}$  of graphene shows quantized plateaux at  $\sigma_{xy} = (2N + 1)e^2/h$  per spin, where  $N$  is an integer. This means that only plateaux with odd number appear and the plateau corresponding to  $\sigma_{xy} = 0$  does not occur. This anomalous QHE originates from the massless Dirac particles realized at the  $K$  and  $K'$  points in the Brillouin zone of graphene.

In our previous study [11], we calculated Chern numbers for realistic multi-band tight-binding models, which describe electrons on graphene. We found that anomalous quantization of Hall conductance persists up to van-Hove singularities, as shown in the previous calculations using simplified model [12]. In addition, the envelope of quantized Hall conductance can be well explained with semi-classical expressions. We further found that the Onsager's quantization rule [13],

$$\frac{S_i(\varepsilon)}{\Omega_{\text{BZ}}} = (n + \gamma)\phi, \quad (2)$$

can predict the positions of plateaux when the band dispersion is well described by single band. Here,  $\phi$  is magnetic flux penetrating in a unit cell and  $\Omega_{\text{BZ}}$  is the area of irreducible Brillouin zone. For Dirac particle regions, above equation also reproduces the positions of Landau levels if we choose Maslov index  $\gamma = 0$ . As this expression does not rely on the linear dispersion of Dirac particles, it can be applicable in wide energy region. Therefore, this expression may be utilized for analysis of QHE and other phenomena of Landau quantization, *e. g.*, de Haas-van Alphen effects.

In this paper, we extend our study to modified version of tight-binding models related to graphene layers. We study how the sequence of Chern numbers may be altered and whether semi-classical rules can be applicable to the extended models.

## 2. Calculation Methods

We describe electrons on honeycomb lattice by tight-binding models. The spin degeneracy is ignored for simplicity. The uniform magnetic field is introduced as phase factors  $\theta_{ij}$  of hoppings so that they satisfy  $\sum_{\text{closed loop}} \theta_{ij} = 2\pi(\text{flux quanta in the loop})$ .

As the original translational symmetry is broken under uniform magnetic field, We must consider magnetic translational symmetry, which is characterized by the magnetic flux  $\phi = B\Omega/\varphi_0$  where  $\Omega$  is the area of a unit cell and  $\varphi_0 = hc/e$  is the quantized magnetic flux. When  $\phi$  is a rational number  $p/q$ , we recover enlarged magnetic unit cell whose area is  $q$  times larger than that of the original cell. Then, eigenstates are labeled by a wave-number  $\mathbf{k}$ . Thus, an energy band splits into  $q$  sub-bands by the uniform field.

Although the Chern number  $c_F$  is given by a sum of the Chern numbers of all filled bands [1], evaluation of them separately causes numerical difficulty since one needs to treat many Chern numbers for the weak field limit, where most of them cancel with each other. Physical Chern number of the filled

Email addresses: arai.masao@nims.go.jp (Masao Arai), hatsugai@sakura.cc.tsukuba.ac.jp (Yasuhiro Hatsugai)

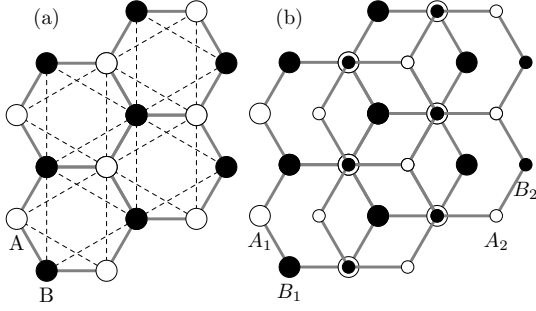


Figure 1: (a) A honeycomb lattice with staggered on-site energies. Two inequivalent sites A and B are distinguished by white and black circles. The dashed lines indicate hoppings between next-nearest sites. (b) A structure model of bilayer graphene. Carbon atoms on upper and lower layer are indicated by small and large circles, respectively.

many body state is stable if the energy gap above the Fermi energy is stable. It is independent of a possible level crossing at far below the Fermi energy. Then the non Abelian formulation of the Chern number by collecting all of the filled bands into a single multiplet  $\Psi$  is quite useful [14, 15, 16]. Then the Chern number  $c_F$  of the multiplet  $\Psi$  is calculated by discretizing the Brillouin zone into mesh  $\{\mathbf{k}_\ell\}$  as [16]

$$\begin{aligned}
 c_F(\mu) &= \frac{1}{2\pi} \sum_{\ell} F(\mathbf{k}_\ell) \\
 F(\mathbf{k}) &= \text{Arg } u_x(\mathbf{k})u_y(\mathbf{k} + \Delta\mathbf{k}_x)[u_x(\mathbf{k} + \Delta\mathbf{k}_y)u_y(\mathbf{k})]^* \\
 u_\mu(\mathbf{k}) &= \det[\Psi(\mathbf{k})]^\dagger \Psi(\mathbf{k} + \Delta\mathbf{k}_\mu) \\
 \Psi(\mathbf{k}) &= (|\psi_1(\mathbf{k})\rangle, \dots, |\psi_M(\mathbf{k})\rangle)
 \end{aligned}$$

where  $\Delta\mathbf{k}_v$  is a discretized momentum along  $v$  direction,  $|\psi_m(\mathbf{k})\rangle$  is a Bloch state of the band index  $m$  and  $m = M$  is the highest occupied energy band below the chemical potential  $\mu$ . This expression can be understood as a two-dimensional analogue of the KSV formula [17].

This formulation was successfully applied to quantum Hall effect on a disorder system[18], graphene[12]. When the field  $\phi = p/q$  is sufficiently small,  $p$  sub-bands are grouped together in general. These grouped bands correspond to a Landau band of nearly free electrons. Hereafter, we treat the field  $\phi = 1/q$ , which enables us to consider the weak-field limit easily.

### 3. Honeycomb lattice with staggered on-site energy

We treat a honeycomb lattice with two inequivalent sites A and B as shown in Fig. 1(a). Single  $\pi$ -orbital is put on each site. The hoppings between nearest and next-nearest neighbor sites are included with parameters  $t_1$  and  $t_2$ . The on-site energies are set to  $\pm\Delta$  for A and B sites. Hereafter, we set  $t_1 = 1$ , i.e.,  $t_1$  is chosen as an energy scale.

When  $t_2 = \Delta = 0$ , this model describes simplified  $\pi$ -bands on graphene and the band dispersions which resemble zero-mass Dirac cones exist at two symmetrically equivalent points,  $K$  ( $1/3$   $1/3$ ) and  $K'$  ( $2/3$   $2/3$ ), in the irreducible Brillouin zone. The QHE of this model has been extensively studied theoretically [12]. Here, we briefly explain the correspondence be-

tween quantum mechanical treatment by Chern numbers and semi-classical quantization rule (2).

The calculated Chern numbers for  $\phi = 1/200$  are plotted as a function of chemical potential in lower panel of Fig. 2. The upper panel shows the total density of states (DOS) when magnetic field is absent. From these figures, we can easily recognize that large discontinuous jumps of Chern numbers correspond to van-Hove singularities at  $\varepsilon = \pm 1$ . Within semi-classical theory, this discontinuity can be explained as a topological transitions of Fermi surface from electron (hole) pockets to hole (electron) pockets[11].

Fig. 3 presents enlarged views of Chern numbers near the van-Hove singularity at  $\varepsilon = 1$ . Anomalous QHE survives up to van-Hove singularities and the sequence of Chern numbers is odd number only, while above singularities Chern numbers change with steps of 1, recovering ordinary QHE [12]. For both regions, semi-classical quantization rule (2) can explain the positions of Landau levels if we choose  $\gamma = 1/2$  at ordinary QHE region and  $\gamma = 0$  at anomalous QHE region. This result is non-trivial near the van-Hove singularity as the band dispersion around  $\varepsilon = 1$  is significantly deformed from the continuum expressions of massless Dirac  $\varepsilon \sim |\mathbf{k}|$  or normal effective mass theory  $\frac{k^2}{2m^*}$ .

We extend our calculations by incorporating next nearest neighbor  $t_2$  and staggered on-site energy  $\pm\Delta$ . When  $\Delta = 0$ , the hoppings  $t_2$  alone do not destroy the massless Dirac cones. In this case, the calculated Chern number sequence remains with  $c_F = \dots, -5, -3, -1, 1, 3, 5, \dots$  as shown in Fig. 4(a). The positions of Landau levels are still explained with the semi-classical quantization with  $\gamma = 0$ .

With finite  $\Delta$ , the Dirac cones at  $K$  and  $K'$  acquire band gaps of order  $2\Delta$ , which means that Dirac particles have finite “mass”. When the chemical potential is located above the gap, Fermi surface is still constructed by two electron pockets around  $K$  and  $K'$ . In addition, the electronic states around  $K$  and  $K'$  are related by lattice symmetry. If we interpret this band structure naively, we may expect that two ordinary electron pockets generate Landau levels at same energies and that Chern numbers between adjacent energy gaps differ by 2. However, we found that such interpretation does not hold for current model. As plotted in Fig. 4(b), additional plateaux appear in  $\sigma_{xy}$  and the Chern numbers increase with steps of 1. In addition, the positions of Landau levels do not agree with semi-classical rule(2) with  $\gamma = 0$  nor  $1/2$ . These results mean that electron pockets near  $K$  and  $K'$  generate Landau levels at different energy positions even though they are equivalent when magnetic field is absent. Indeed, the positions of Landau levels may be explained if we choose different  $\gamma$  for Fermi surface segments around  $K$  and  $K'$ .

### 4. Bilayer graphene

The graphene bilayer consists of two honeycomb lattices as shown in Fig. 1(b). Each layer is composed of two inequivalent sites which we denote  $A_1$  and  $B_1$  on lower layer, and  $A_2$  and  $B_2$  on upper one. The  $B_2$  sites on upper layer are located above

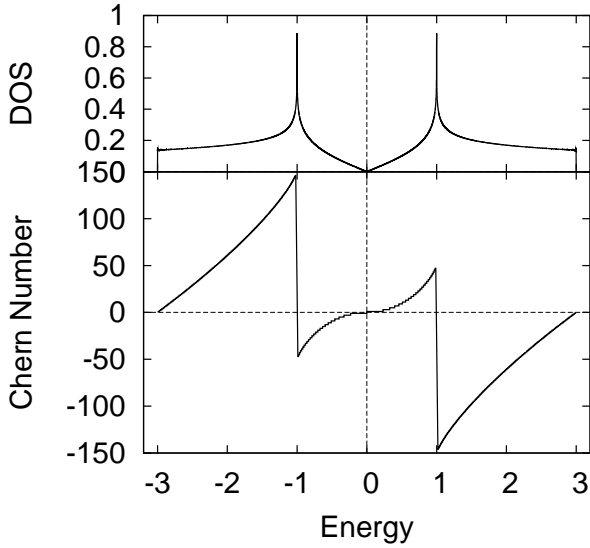


Figure 2: The upper panel shows the total density of states (DOS) without magnetic field. The lower panel presents calculated Chern number sequence as a function of chemical potential.

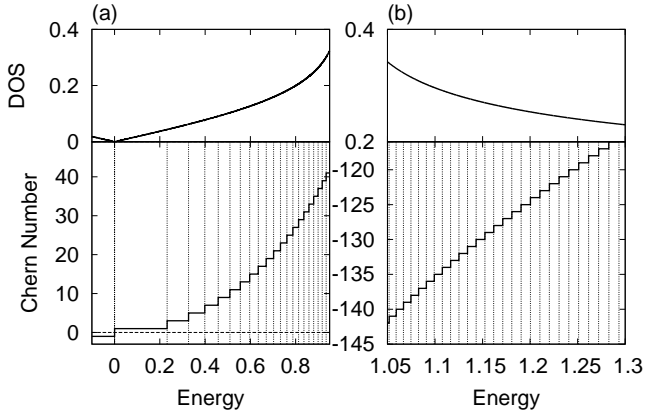


Figure 3: The upper panel shows the total density of states (DOS) without magnetic field. The lower panel presents calculated Chern number sequence as a function of chemical potential. The vertical dashed lines indicate the positions where semi-classical quantization rule is satisfied with (a)  $\gamma = 0$  and (b)  $\gamma = 1/2$ .

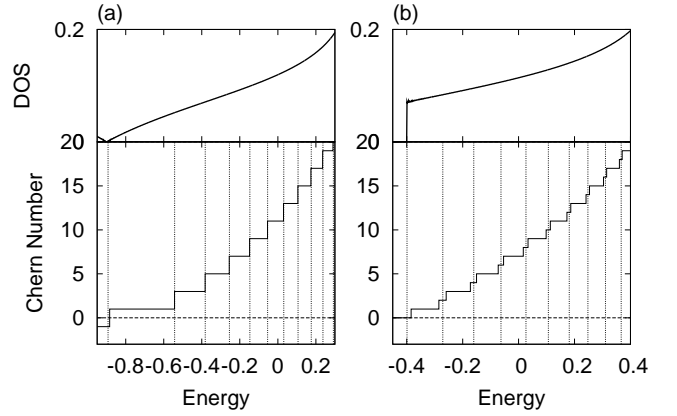


Figure 4: The total DOS and Chern numbers for a honeycomb lattice model. The magnetic field is  $\phi = 1/101$ . The dashed lines indicate the positions where semi-classical quantization rule is satisfied with  $\gamma = 0$ . (a)  $\Delta = 0$ ,  $t_2 = 0.3$ . (b)  $\Delta = 0.5$ ,  $t_2 = 0.3$ .

the  $A_1$  sites on lower layer. The largest hoppings  $\gamma_0$  between  $\pi$ -orbitals are between nearest-neighbor atoms on the same layer. The inter-layer hoppings are included between  $A_1$  and  $B_2$  sites with parameter  $\gamma_1$ . Other hoppings are ignored for simplicity. These parameters are taken from previous estimations [19] as  $\gamma_0 = 2.6\text{eV}$  and  $\gamma_1/\gamma_0 \approx 0.14$ .

The QHE of bilayer graphene was observed experimentally [20] and its electronic structure has been studied extensively [21, 22, 23]. Within the present model, the electron-hole symmetry is maintained and band dispersions are symmetric around  $\varepsilon = 0$ . The inter-layer hoppings modify the Dirac cones which exist in single-graphene and results in two branches of energy bands for  $\varepsilon > 0$ . Both branches behave as  $\varepsilon = \delta k^2$  near the  $K$  and  $K'$  points. In addition, the lower branches remain gapless.

The uniform magnetic field is applied along perpendicular to layers. Fig. 5 shows global structure of calculated Chern numbers as a function of chemical potential. The total DOS without magnetic field is also plotted with same energy scale. Because two branches of energy bands exist, pair of van-Hove singularities appear around  $\varepsilon = \pm 1$ . Accordingly, the large discontinuous jumps of Chern numbers around  $\varepsilon = \pm 1$  split into two jumps. At  $\varepsilon = 0$ , the Chern numbers jump from -2 to 2, suggesting the existence of 4 Landau levels at  $\varepsilon = 0$ . The positions of other Landau levels shown in Fig. 6(a) seem to be located without concrete rule. This is because both upper and lower branches of energy bands contribute to the quantized Landau levels. Nonetheless, the Chern numbers always jump by 2, which results in the sequence of  $c_F = \dots, -4, -2, 2, 4, \dots$ .

We studied Landau levels from lower branch of energy bands by lifting the upper branch with large  $\gamma_1$ . Fig. 6(b) shows the sequence of Chern numbers with  $\gamma_1/\gamma_0 = 0.6$ . With this parameter, only lower branch with gapless dispersion contributes to quantized Landau levels near  $\varepsilon = 0$ . As a result, the appearance of Landau levels becomes systematic but can not be explained by standard semi-classical rule irrespective to the choice of  $\gamma$ . In the continuum limit, analytical expression of Landau levels

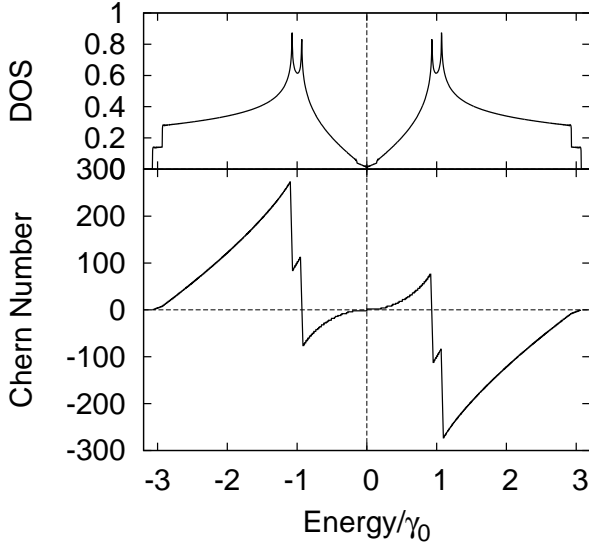


Figure 5: The total DOS (upper panel) and Chern number sequences for bilayer graphene are shown.

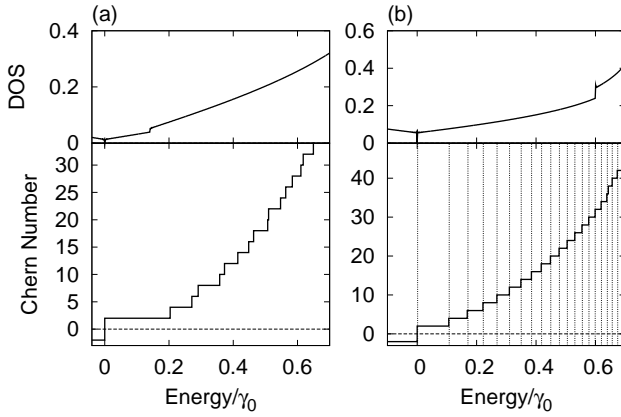


Figure 6: The total DOS and Chern numbers for bilayer honeycomb lattice. Parameters are chosen as (a)  $\gamma_1/\gamma_0 = 0.14$  and (b)  $\gamma_1/\gamma_0 = 0.6$ . The vertical lines indicate the positions of Landau levels calculated from modified semi-classical rule (2).

has been obtained as  $\varepsilon \sim \sqrt{n(n-1)}$  [21]. Using this expression as a guide, we have tried several modifications to the semi-classical rule and found that the equation

$$\frac{S_i(\varepsilon)}{\Omega_{\text{BZ}}} = \sqrt{n(n-1)}\phi \quad (3)$$

agrees with calculated Landau levels within the energy scale presented in Fig. 6(b). However, we have not found any theoretical support for above equation. Further studies would be necessary to clarify the quantization rule.

## 5. Conclusion

We studied quantum Hall effect on single and bilayer honeycomb lattices. For single-layer honeycomb lattice without staggered on-site energies, the semi-classical theory explains the

position of Landau level if we choose  $\gamma$  appropriately. When the on-site energies are introduced, additional plateaux will appear. This indicates that valley degeneracy between  $K$  and  $K'$  is broken when the magnetic field is applied.

For bilayer graphene, the Chern number sequence of  $c_F = \dots, -4, -2, 2, 4, 6, \dots$  is obtained, which agrees with previous theoretical results. The semi-classical interpretation is difficult when multiple bands contribute to the same energy regions.

This research by MA is partially supported by a Grant-in-Aid for Scientific Research, No. 18540331 and No. 17064016 from JSPS. The work by YH is also supported in part by Grants-in-Aid for Scientific Research, No. 20340098 and No. 20654034 from JSPS, No. 220029004 (physics of new quantum phases in super clean materials) and 20046002 (Novel States of Matter Induced by Frustration) on Priority Areas from MEXT.

## References

- [1] D. J. Thouless, M. Kohmoto, M. P. Nightingale, M. den Nijs, Phys. Rev. Lett. **49** (1982) 405.
- [2] P. Streda, J. Phys. C **15** (1982) L717.
- [3] M. Kohmoto, Ann. Phys. **160** (1985) 343.
- [4] Q. Niu, D. J. Thouless, Y.-S. Wu, Phys. Rev. B **31** (1985) 3372.
- [5] H. Aoki, T. Ando, Phys. Rev. Lett. **57** (1986) 3093.
- [6] B. I. Halperin, Phys. Rev. B **25** (1982) 2185.
- [7] Y. Hatsugai, Phys. Rev. Lett. **71** (1993) 3697.
- [8] Y. Hatsugai, Phys. Rev. B **48** (1993) 11851.
- [9] K. S. Novoselov, E. McCann, S. V. Morozov, V. I. Fal'ko, M. I. Katsnelson, V. Zeitler, D. Jiang, F. Schedin, A. K. Geim, Nature **438** (2005) 197.
- [10] Z. Zhang, Y.-W. Tan, H. L. Stormer, P. Kim, Nature **438** (2005) 201.
- [11] M. Arai, Y. Hatsugai, Phys. Rev. B **79** (2008) 075429.
- [12] Y. Hatsugai, T. Fukui, H. Aoki, Phys. Rev. B **74** (2006) 205414.
- [13] L. Onsager, Philos. Mag. **43** (1952) 1006.
- [14] Y. Hatsugai, J. Phys. Soc. Jpn. **73** (2004) 2604.
- [15] Y. Hatsugai, J. Phys. Soc. Jpn. **74** (2005) 1374.
- [16] T. Fukui, Y. Hatsugai, H. Suzuki, J. Phys. Soc. Jpn. **74** (2005) 1674.
- [17] R. D. King-Smith, D. Vanderbilt, Phys. Rev. B **47** (1993) 1651.
- [18] H. Song, I. Maruyama, Y. Hatsugai, Phys. Rev. B **76** (2007) 132202.
- [19] J.-C. Charlier, J.-P. Michenaud, X. Gonze, J.-P. Vigneron, Phys. Rev. B **44** (1991) 13237.
- [20] K. S. Novoselov, E. McCann, S. V. Morozov, V. I. Fal'ko, M. I. Katsnelson, V. Zeitler, D. Jiang, F. Schedin, A. K. Geim, Nature Phys. **2** (2006) 177.
- [21] E. McCann, V. I. Fal'ko, Phys. Rev. Lett. **96** (2006) 086805.
- [22] F. Guinea, A. H. Castro Neto, N. M. R. Peres, Phys. Rev. B **73** (2006) 245426.
- [23] M. Koshino, T. Ando, Phys. Rev. B **73** (2006) 245403.